Journal of Math-for-Industry, Vol. 3 (2011C-6), pp. 41–51

Math-for-industry
Education & Research Hub

Application of the nonlinear Galerkin FEM method to the solution of the reaction diffusion equations

Jan Mach

Revised on November 5, 2011

Abstract. The article summarizes application of the nonlinear Galerkin method to the numerical solution of reaction-diffusion systems - the Gray-Scott model and simplified equation. The space discretization is performed by the finite-element method. For time integration we use the Runge-Kutta method with time step adaptivity. The computational results demonstrate properties of the method and the comparison with the finite difference method.

Keywords. Nonlinear Galerkin method, Gray-Scott model, reaction-diffusion equation, method of lines, finite difference method, finite element method, Runge-Kutta-Merson method.

1. Introduction

Consider the system of reaction-diffusion equations

$$\frac{\partial U}{\partial t} = \mathbf{D}\Delta U + \mathbf{F}(U), \tag{1}$$

where $\mathbf{D} \in \mathbb{R}^{d,d}$ denotes a positively definite diagonal matrix, $\mathbf{F} : \mathbb{R}^d \to \mathbb{R}^d$ is a Lipschitz continuous mapping, $U(t,z)$ is a d-dimensional function of time $t \geq 0$ and of space $z \in \Omega \subset \mathbb{R}^n$. Ω is a bounded space domain with piecewise smooth boundary. We consider the homogeneous Neumann boundary conditions

$$\frac{\partial U}{\partial \nu} = 0, \tag{2}$$

where ν is the unit outward normal on Ω and the initial condition

$$U|_{t=0} = U_0 \in \mathbf{H}, \tag{3}$$

where $\mathbf{H} := \mathbf{L}^2(\Omega, \mathbb{R}^d)$ is the Hilbert space with the scalar product

$$(U,V) \equiv (U,V)_{\mathbf{H}} = \sum_{i=1}^{d} (U_i, V_i)_{\mathbf{H}} = \sum_{i=1}^{d} \int_\Omega U_i V_i, \tag{4}$$

and the space $\mathbf{V} := \mathbf{H}^{(1)}(\Omega, \mathbb{R}^d)$ as a Hilbert space with the bilinear form

$$(U,V)_{\mathbf{V}} = \sum_{i=1}^{d} (U_i, V_i)_{\mathbf{H}^{(1)}(\Omega)} = \sum_{i=1}^{d} \int_\Omega \nabla U_i \cdot \nabla V_i, \tag{5}$$

where $U = (U_1, \ldots, U_d)$, $V = (V_1, \ldots, V_d)$.

The weak solution of the problem (1)-(3) on the time interval $(0,T)$ is a mapping $U : (0,T) \to \mathbf{V}$ such that it satisfies the following conditions:

$$\frac{\mathrm{d}}{\mathrm{d}t}(U,W) + (\mathbf{D}U, W)_{\mathbf{V}} = (\mathbf{F}(U), W) \quad \text{in } (0,T)\ \forall W \in \mathbf{V}, \tag{6}$$

$$U|_{t=0} = U_0. \tag{7}$$

The article is organized as follows. In section 2 we present the error estimate for a class of commonly used numerical schemes. The finite element nonlinear Galerkin scheme is derived in section 3. In section 4 we apply this method to the Gray-Scott reaction-diffusion system. In section 5 we present results of our numerical simulations for the Gray-Scott model and simplified equation with analytical solution. We compare numerical results by the nonlinear Galerkin approaches with those by the standard finite difference scheme. We performed quantitative comparison of numerical results, CPU time consumption comparison and computational efficiency measurement for tested numerical schemes.

2. Conventional Error estimate

As a part of motivation, we derive the error estimate for one of the commonly used numerical schemes. Let U be the exact solution of the problem (1) - (3) in one spatial dimension. Consider the following numerical scheme based on the finite difference method,

$$\frac{\mathrm{d}}{\mathrm{d}t} U_h = \mathbf{D}U_{h\overline{x}x} + \mathbf{F}(U_h). \tag{8}$$

Denote $\mathcal{P}_h$ the projector (restriction) on the numerical grid and define the approximation error ψ for the second derivative,

$$\psi_h = \mathcal{P}_h \mathbf{D} \partial^2_{xx} U - \mathbf{D}(\mathcal{P}_h U)_{\overline{x}x}.$$

Denote $\overline{\omega}_h = \{jh | j = 0, \ldots, n\}$, $n \in \mathbb{N}$ the grid of points in $[0, L]$, where $h = \frac{L}{n}$. We use notation U_i^j for a component i of the solution vector U evaluated at numerical grid node j. Then the backward and forward differences, respectively, are

$$U_{i,\overline{x}}^j = \frac{U_i^j - U_i^{j-1}}{h}$$

and

$$U_{i,x}^j = \frac{U_i^{j+1} - U_i^j}{h}.$$

The second derivative is approximated by $(\partial_{xx}^2 U_i)^j \sim U_{i,\overline{x}x}^j$. For vector grid functions U_h, V_h we denote scalar products

$$(U_h, V_h)_h = \sum_{k=1}^{d} \sum_{m=1}^{n-1} h U_{h,k}^m V_{h,k}^m,$$
$$(U_h, V_h]_h = \sum_{k=1}^{d} \sum_{m=1}^{n} h U_{h,k}^m V_{h,k}^m,$$

and corresponding norms

$$\|U_h\|_h = \sqrt{(U_h, U_h)_h},$$
$$\|U_h]|_h = \sqrt{(U_h, U_h]_h}.$$

Subtracting (1) from (8) on the numerical grid we get

$$\frac{\mathrm{d}}{\mathrm{d}t}(U_h - \mathcal{P}_h U) = \mathbf{D}(U_h - \mathcal{P}_h U)_{\overline{x}x} + \mathbf{F}(U_h) - \mathcal{P}_h \mathbf{F}(U) - \psi_h.$$

Multiplying by $E = U_h - \mathcal{P}_h U$ we further derive

$$\frac{1}{2}\frac{\mathrm{d}}{\mathrm{d}t}\|E\|_h^2 + \mathbf{D}\|E_{\overline{x}}]|_h^2 = (F(U_h) - \mathcal{P}_h F(U), E)_h + (\psi_h, E)_h + (\tilde{\psi}_h, E)_h,$$

where $\tilde{\psi}_h$ is a term coming from approximation of the Neumann boundary conditions. Lipschitz continuity of the mapping $\mathbf{F}$ gives

$$|(\mathbf{F}(U_h) - \mathcal{P}_h \mathbf{F}(U), E)_h| \quad \leq \quad C\|E\|_h^2.$$

Next, using the Schwarz inequality and the Young inequality and the estimate (9) in (9) we get

$$\begin{aligned} \frac{1}{2}\frac{\mathrm{d}}{\mathrm{d}t}\|E\|_h^2 &\leq C\|E\|_h^2 + \|\psi_h\|_h^2 + 2\|E\|_h^2 + \|\tilde{\psi}_h\|_h^2 \\ &\leq K\|E\|_h^2 + \mathcal{O}(h^2) + \|\tilde{\psi}_h\|_h^2, \end{aligned}$$

where $C > 0$, $K > 0$ are positive constants. Finally, application of the Gronwall inequality gives estimate of the approximation error in the form

$$\|E\|_h^2(t) \leq (\|E\|_h^2(0) + \mathcal{O}(h^2) + \|\tilde{\psi}_h\|_h^2) \exp(KT).$$

3. Nonlinear multiscale scheme

Complex long-term dynamics of reaction-diffusion problems requires finer approach to quantitatively reliable numerical schemes, for which the error estimate constant does not grow with T. One of approaches is known as the nonlinear Galerkin method and was introduced in 1989 by M. Marion and R. Temam [5]. The motivation for this method was to capture the effect of some of the terms that are neglected in the usual Galerkin method, where approximation of the solution is searched in the space spanned by basis functions $w_1, \ldots, w_m$ neglecting terms in the orthogonal space.

For the nonlinear Galerkin method a basis of $2m$ (may be generalized to cm, where $c \in \mathbb{N}$, $c > 2$) functions $w_1, \ldots, w_{2m}$ is considered. The solution U of the problem (1) - (3) is approximated by U_m

$$U_m(t, z) \quad = \quad \sum_{j=1}^{m} G_{jm}(t) w_j(z), \tag{9}$$

with a correction term Z_m

$$Z_m(t, z) \quad = \quad \sum_{j=m+1}^{2m} H_{jm}(t) w_j(z). \tag{10}$$

Coefficients U_m and Z_m satisfy the system of equations

$$\frac{\partial U_m}{\partial t}(t, z) \quad = \quad P_m F(U_m(t, z) + Z_m(t, z)), \tag{11}$$

$$\begin{aligned} 0 \quad = \quad & (P_{2m} - P_m)(F(U_m(t, z)) + \\ & F^{'}(U_m(t, z)) \cdot (Z_m(t, z))), \end{aligned} \tag{12}$$

where P_j is the orthogonal projector onto the space spanned by $w_1, \ldots, w_j$ in the underlying Hilbert space $H := L^2(\Omega, \mathbb{R}^d)$, $F^{'}$ is the derivative with respect to argument components of F.

At each time t, the values of $Z_m(t)$ are expected to be nearly negligible. The effect of $Z_m(t)$ adds up and is effective on large intervals of time.

The semi-discrete scheme (11) - (12) was analyzed in [5] for a class of nonlinear evolution problems covering the Navier-Stokes equations, and in [12] for reaction-diffusion systems admitting invariant regions. In both papers Fourier spectral discretization is used.

The idea of the nonlinear Galerkin method is further extended to finite element method in [6] for the same class of problems as in [5]. In [7] an error estimate is induced, which shows that when the ration between coarse and fine grid mesh sizes is chooses appropriately, the nonlinear Galerkin and standard Galerkin method provide the same order of approximation. Its shown that the relation between coarse grid size H and fine grid size h needs to be $H = O(h^{1/3})$ in this case. In this paper we use $H = 2h$, which is used, e.g., in the example application of the method in [6].

Numerical studies show computational properties of the nonlinear Galerkin method in the context of finite element discretization. For example, numerical tests in [4]

show that the nonlinear Galerkin method is superior to the standard Galerkin method for the numerical solution of the penalized Navier-Stokes equations. For numerical study of several forms of the nonlinear Galerkin scheme see [9], where these schemes are applied for the numerical solution of one-dimensional Burgers and Kuramoto-Sivashinsky equations. Within conclusions it says, that these schemes may be useful if high accuracy is required for the approximate solution.

In the finite element nonlinear Galerkin method multigrid discretization and hierarchical bases are used to follow the definition of U_m, Z_m in (9), (10). Here, we restrict

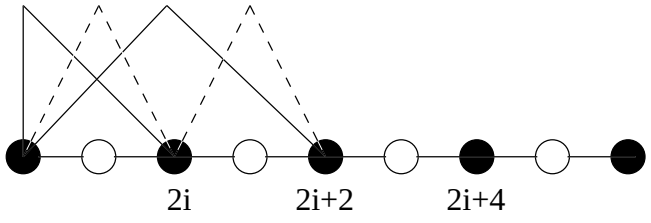

Figure 1: Basis functions at odd and even grid nodes in 1D.

ourselves to one spatial dimension, $\Omega \subset \mathbb{R}$, and consider two level discretization, one with mesh parameter $2h$ and the second twice finer with mesh parameter h, see Fig. 1. Following the procedure in [6], we set $n = 2m + 1$ and define finite element piecewise linear basis functions ψ_{2i+1} (doted line) at grid nodes x_{2i+1}, $i = 0, \ldots, m-1$ and basis functions φ_{2i} (solid line) at grid nodes x_{2i}, $i = 0, \ldots, m$. We define

$$\left[\varphi_{2i}^{(1)} = \begin{pmatrix} \varphi_{2i} \\ 0 \\ \vdots \\ 0 \end{pmatrix}, \ldots, \varphi_{2i}^{(d)} = \begin{pmatrix} 0 \\ \vdots \\ 0 \\ \varphi_{2i} \end{pmatrix} \right]_{i=0}^{m},$$

$$\left[\psi_{2i+1}^{(1)} = \begin{pmatrix} \psi_{2i+1} \\ 0 \\ \vdots \\ 0 \end{pmatrix}, \ldots, \psi_{2i+1}^{(d)} = \begin{pmatrix} 0 \\ \vdots \\ 0 \\ \psi_{2i+1} \end{pmatrix} \right]_{i=0}^{m-1},$$

as d-dimensional vector-valued finite element basis functions and set

$$V_{2h} = Span\{\varphi_0^{(1)}, \ldots, \varphi_0^{(d)}, \ldots, \varphi_{2m}^{(1)}, \ldots, \varphi_{2m}^{(d)}\},$$

$$W_h = Span\{\psi_1^{(1)}, \ldots, \psi_1^{(d)}, \ldots, \psi_{2m-1}^{(1)}, \ldots, \psi_{2m-1}^{(d)}\}.$$

Next we define the space V_h by

$$V_h = Span\{\varphi_0^{(1)}, \ldots, \varphi_0^{(d)}, \ldots, \varphi_{2m}^{(1)}, \ldots, \varphi_{2m}^{(d)}, \psi_1^{(1)}, \ldots, \psi_1^{(d)}, \ldots, \psi_{2m-1}^{(1)}, \ldots, \psi_{2m-1}^{(d)}\}.$$

Solution of the problem (6) - (7) is approximated by

$$\tilde{U}_m(t) \quad = \quad U_m(t) + Z_m(t),$$

where functions U_m, Z_m are given as

$$U_m(t) \quad = \quad \sum_{i=0}^{m} \sum_{l=1}^{d} u_{2i}^{(l)}(t) \varphi_{2i}^{(l)} \in V_{2h}, \tag{13}$$

$$Z_m(t) \quad = \quad \sum_{i=0}^{m-1} \sum_{l=1}^{d} z_{2i+1}^{(l)}(t) \psi_{2i+1}^{(l)} \in W_h. \tag{14}$$

and have to satisfy the following set of equations

$$\begin{aligned} &\frac{\mathrm{d}}{\mathrm{d}t}(U_m(t), \varphi_{2i}^{(l)}) + (\mathbf{D}U_m(t), \varphi_{2i}^{(l)})_{\mathbf{V}} = \\ &\qquad (\mathbf{F}(U_m(t) + Z_m(t)), \varphi_{2i}^{(l)}), \qquad (15) \\ &\qquad i = 0, \ldots, m | l = 1, \ldots, d, \\ &(\mathbf{D}Z_m(t), \psi_{2i+1}^{(l)})_{\mathbf{V}} = \\ &\qquad (\mathbf{F}(U_m(t)) + \nabla \mathbf{F}(U_m(t)) Z_m(t), \psi_{2i+1}^{(l)}), \qquad (16) \\ &\qquad i = 0, \ldots, m-1 | l = 1, \ldots, d, \\ &(U_m(0), \varphi_{2i}^{(l)}) = (U_0, \varphi_{2i}^{(l)}), \\ &\qquad i = 0, \ldots, m | l = 1, \ldots, d. \end{aligned}$$

The existence and uniqueness of the solution of the problem (15) - (16) follows from the standard theorems on the Cauchy problem for the ordinary differential equations.

Convergence of the finite element nonlinear Galerkin method for a system of reaction-diffusion equations will be rigorously shown elsewhere. Convergence of method for a different problem is discussed in [6].

4. Application to particular reaction-diffusion models

In this section we present results of our numerical simulations and compare numerical schemes based on the finite element nonlinear Galerkin method (15) - (16) and the finite difference method applied to the numerical solution of selected reaction-diffusion equations, the Gray-Scott model and simplified equation with known analytical solution, in one spatial dimension.

Numerical studies show that it is not always easy to approximate the dynamics of the model (1). We compare two numerical approaches for solution of the initial-boundary value problem for selected reaction-diffusion equations in order to disclose details of these problems.

The first test model is the Gray-Scott model, which was introduced in 1984 by P. Gray and S. K. Scott [3]. It is a mathematical model of the autocatalytic chemical reaction

$$U + 2V \to 3V, \quad V \to P, \tag{17}$$

where U, V are reactants and P is final product of the reaction. Chemical substance U is being continuously added into the reactor and the product P is being continuously removed from the reactor during the reaction. Later the model has been extensively studied, e.g., by Wei [14], Winter [13], Ueyama [10], Dkhil [1], Doelman [2]. This model is well known to exhibit rich dynamics, as shown in Nishiura [11].

The chemical reaction (17) may be rewritten as a system of two PDEs of parabolic type in several dimensionless forms. We use the one which is used also, e.g., in [13, 8]. Here we focus on the Gray-Scott model in one spatial dimension. Assume that $\Omega \equiv (0, L)$ represents the reactor, where the chemical reaction takes place, $\partial\Omega$ is boundary of Ω and ν is the unit outward normal on Ω. Then the initial-boundary value problem for the Gray-Scott model is the following system:

$$\frac{\partial u}{\partial t} = D_u \Delta u - uv^2 + F(1-u), \tag{18}$$

$$\frac{\partial v}{\partial t} = D_v \Delta v + uv^2 - (F+k)v, \tag{19}$$

in $\Omega \times (0, T)$ with initial conditions

$$u(\cdot, 0) = u_{ini}, \tag{20}$$

$$v(\cdot, 0) = v_{ini} \tag{21}$$

and zero Neumann boundary conditions

$$\frac{\partial u}{\partial \nu} |_{\partial\Omega} = 0, \tag{22}$$

$$\frac{\partial v}{\partial \nu} |_{\partial\Omega} = 0. \tag{23}$$

Functions u, v are unknowns representing concentrations of chemical substances U, V. Parameter F denotes the rate at which the chemical substance U is being added during the chemical reaction, $F + k$ is the rate of $V \to P$ transformation and a, b are constants characterizing the environment of the reactor. We denote right-hand sides in the system (18)-(19) by $F_1(u, v) = F(1-u) - uv^2$, $F_2(u, v) = -(F+k)v + uv^2$ (or F_1, F_2 only).

The finite element nonlinear Galerkin method is applied to the solution of the Gray-Scott model as follows. The system (15) - (16) reads as

$$\partial_t(u_m(t), \varphi_{2i}) + D_u(u_m(t), \varphi_{2i})_{\mathbf{V}} = (F_1(u_m(t) + z_m(t), v_m(t) + w_m(t)), \varphi_{2i}), \tag{24}$$

$$\partial_t(v_m(t), \varphi_{2i}) + D_v(v_m(t), \varphi_{2i})_{\mathbf{V}} = (F_2(u_m(t) + z_m(t), v_m(t) + w_m(t)), \varphi_{2i}), \quad i = 0, \ldots, m; \tag{25}$$

$$D_u(z_m(t), \psi_{2i+1})_{\mathbf{V}} = (F_1(u_m(t), v_m(t)) + \partial_u F_1(u_m(t), v_m(t)) z_m(t) + \partial_v F_1(u_m(t), v_m(t)) w_m(t), \psi_{2i+1}), \tag{26}$$

$$D_v(w_m(t), \psi_{2i+1})_{\mathbf{V}} = (F_2(u_m(t), v_m(t)) + \partial_u F_2(u_m(t), v_m(t)) z_m(t) + \partial_v F_2(u_m(t), v_m(t)) w_m(t), \psi_{2i+1}), \quad i = 0, \ldots, m-1; \tag{27}$$

where u_m, v_m are numerical approximations of the solution:

$$u_m(t) = \sum_{i=0}^{m} u_{2i}(t)\varphi_{2i}, \tag{28}$$

$$v_m(t) = \sum_{i=0}^{m} v_{2i}(t)\varphi_{2i}, \tag{29}$$

and z_m, w_m corresponding correction terms:

$$z_m(t) = \sum_{i=0}^{m-1} z_{2i+1}(t)\psi_{2i+1}, \tag{30}$$

$$w_m(t) = \sum_{i=0}^{m-1} w_{2i+1}(t)\psi_{2i+1}. \tag{31}$$

Equations for unknowns z_{2i+1}, w_{2i+1} in (30), (31) are induced as follows. Numerical integrations is used to approximate right-hand sides in equations (26), (27). For $j = 1, 2$ and $i = 0, \ldots, m-1$ we have

$$(F_j + \partial_u F_1 z_m + \partial_v F_1 w_m, \psi_{2i+1}) \sim hF_j|_{2i+1} + h\partial_u F_1|_{2i+1} z_{2i+1} + h\partial_v F_1|_{2i+1} w_{2i+1},$$

and for $i = 0, \ldots, m-1$ we get

$$(z_m(t), \psi_{2i+1})_{\mathbf{V}} = \frac{2}{h} z_{2i+1},$$

$$(w_m(t), \psi_{2i+1})_{\mathbf{V}} = \frac{2}{h} w_{2i+1}.$$

Finally, we derive equations for corrections

$$D_u \frac{2}{h^2} z_{2i+1} = F_1|_{2i+1} + \partial_u F_1|_{2i+1} z_{2i+1} + \partial_v F_1|_{2i+1} w_{2i+1},$$

$$D_v \frac{2}{h^2} w_{2i+1} = F_2|_{2i+1} + \partial_u F_2|_{2i+1} z_{2i+1} + \partial_v F_2|_{2i+1} w_{2i+1}.$$

This is a linear system with 2×2 matrix

$$\begin{pmatrix} D_u \frac{2}{h^2} - \partial_u F_1|_{2i+1} & -\partial_v F_1|_{2i+1} \\ -\partial_u F_2|_{2i+1} & D_v \frac{2}{h^2} - \partial_v F_2|_{2i+1} \end{pmatrix}$$

for corrections z_{2i+1}, w_{2i+1} at the grid point x_{2i+1} with right-hand side vector $(F_1|_{2i+1}, F_2|_{2i+1})$, which we solve by the Cramer's rule.

The systems of equations for unknown functions u_{2i}, v_{2i} in (28), (29) is induced as follows. Numerical integrations is used to approximate terms (F_j, φ_{2i}) for $j = 1, 2$ in equations (24), (25)

$$(F_j, \varphi_{2i}) \sim \frac{h}{2} F_j|_{2i-1} + hF_j|_{2i} + \frac{h}{2} F_j|_{2i+1},$$

for $i = 1, \ldots, m-1$. For $i = 0$ and $i = m$ we have

$$(F_j, \varphi_0) \sim \frac{h}{2} F_j|_0 + \frac{h}{2} F_j|_1,$$

and

$$(F_j, \varphi_{2m}) \sim \frac{h}{2} F_j|_{2m-1} + \frac{h}{2} F_m|_{2m}$$

respectively. Defining a $(m+1) \times (m+1)$ mass matrix $\mathcal{M} \equiv ((\varphi_{2l}, \varphi_{2k}))_{l,k=0}^{m}$ and denoting vectors of unknowns $\dot{u} = (\dot{u}_0, \ldots, \dot{u}_{2m})$, $\dot{v} = (\dot{v}_0, \ldots, \dot{v}_{2m})$ we can write equations (24), (25) in the form of linear systems with tridiagonal matrix $\mathcal{M}$

$$\mathcal{M}\dot{u} = b_u, \tag{32}$$

$$\mathcal{M}\dot{v} = b_v, \tag{33}$$

which we solve by the tridiagonal matrix algorithm - a simplified form of Gaussian elimination. Numerical results by the numerical algorithm involving solution of linear systems (32), (33) are denoted as *tridiag*. Using mass-lumping we can write systems (32), (33) in the form

$$\begin{aligned}
\frac{\mathrm{d}}{\mathrm{d}t}u_0 &= \frac{D_u}{2h^2}(-u_0+u_2)+\frac{1}{2}F_1|_0+\frac{1}{2}F_1|_1, && (34)\\
\frac{\mathrm{d}}{\mathrm{d}t}v_0 &= \frac{D_v}{2h^2}(-v_0+v_2)+\frac{1}{2}F_2|_0+\frac{1}{2}F_2|_1, && (35)\\
\frac{\mathrm{d}}{\mathrm{d}t}u_{2i} &= \frac{D_u}{4h^2}(u_{2i+2}-2u_{2i}+u_{2i-2})+\\
&\quad \frac{1}{4}F_1|_{2i+1}+\frac{1}{2}F_1|_{2i}+\frac{1}{4}F_1|_{2i-1}, && (36)\\
\frac{\mathrm{d}}{\mathrm{d}t}v_{2i} &= \frac{D_v}{4h^2}(v_{2i+2}-2v_{2i}+v_{2i-2})+\\
&\quad \frac{1}{4}F_2|_{2i+1}+\frac{1}{2}F_2|_{2i}+\frac{1}{4}F_2|_{2i-1}, && (37)\\
&\quad i=1,\ldots,m-1,\\
\frac{\mathrm{d}}{\mathrm{d}t}u_{2m} &= \frac{D_u}{2h^2}(-u_{2m}+u_{2m-2})+\\
&\quad \frac{1}{2}F_1|_{2m-1}+\frac{1}{2}F_1|_{2m}, && (38)\\
\frac{\mathrm{d}}{\mathrm{d}t}v_{2m} &= \frac{D_v}{2h^2}(-v_{2m}+v_{2m-2})+\\
&\quad \frac{1}{2}F_2|_{2m-1}+\frac{1}{2}F_2|_{2m}. && (39)
\end{aligned}$$

Numerical results by the numerical algorithm involving solution of (34) - (39) are denoted *nomat*.

For time integration we use in both cases Runge-Kutta-Merson method, modified Runge-Kutta method with time step adaptivity. At each step of Runge-Kutta-Merson method we first compute compute corrections z_m, w_m which are then used to compute the coefficients of the Runge-Kutta method in either (32) - (33) or (34) - (39) when evaluating the F_1, F_2 terms. Linear interpolation is used when evaluating properties $u_m + z_m$ and $v_m + w_m$ to get values of u_m, v_m at grid nodes x_{2i+1}, $i = 0, \ldots, m-1$.

For comparison we use the numerical scheme based on the finite difference method:

$$\begin{aligned}
\frac{\mathrm{d}}{\mathrm{d}t}u_0 &= \frac{D_u}{h^2}(-2u_0+2u_1)+F_1|_0, && (40)\\
\frac{\mathrm{d}}{\mathrm{d}t}v_0 &= \frac{D_v}{h^2}(-2v_0+2v_1)+F_2|_0, && (41)\\
\frac{\mathrm{d}}{\mathrm{d}t}u_i &= \frac{D_u}{h^2}(u_{i-1}-2u_i+u_{i+1})+F_1|_i, && (42)\\
\frac{\mathrm{d}}{\mathrm{d}t}v_i &= \frac{D_v}{h^2}(v_{i-1}-2v_i+v_{i+1})+F_2|_i, && (43)\\
&\quad i=1,\ldots,2m-1.\\
\frac{\mathrm{d}}{\mathrm{d}t}u_{2m} &= \frac{D_u}{h^2}(2u_{2m-1}-2u_{2m})+F_1|_{2m}, && (44)\\
\frac{\mathrm{d}}{\mathrm{d}t}v_{2m} &= \frac{D_v}{h^2}(2v_{2m-1}-2v_{2m})+F_2|_{2m}. && (45)
\end{aligned}$$

Corresponding numerical results are denoted *fdm*.

We also applied the finite element nonlinear Galerkin method to the numerical solution of a simplified reaction diffusion equation with known analytic solution. Namely, we consider the function $u(t,x) = sin(\alpha t)cos(\beta x) + \gamma$ for real constants α, β, γ and require it to solve the equation

$$\partial_t u = D\Delta u + f(u) + g(t,x). \qquad (46)$$

Inserting function u into the equation (46), we obtain the formula for the right-hand side $g(t,x)$. Then u solves the initial-boundary value problem

$$\begin{aligned}
\partial_t u &= D\Delta u + f(u) + g(t,x)\\
&\quad \text{on } (0,+\infty)\times(0,L),\\
\partial_x u(t,0) &= 0,\ \partial_x u(t,L) = 0, && (47)\\
u|_{t=0} &= \gamma,
\end{aligned}$$

when $\beta = \pi k/L$, $k \in \mathcal{Z}$. In particular, for $f(u) = u^2$ we have

$$\begin{aligned}
g(t,x) &= \alpha cos(\alpha t)cos(\beta x) + D\beta^2 sin(\alpha t)cos(\beta x) -\\
&\quad (sin(\alpha t)cos(\beta x)+\gamma)^2.
\end{aligned}$$

Analogy of numerical schemes (32) - (33), (34) - (39) and (40) - (45) were induced to solve the problem (47).

5. Numerical results

Numerical simulations for the Gray-Scott model presented here were performed for the following parameters exhibiting nontrivial behavior of solutions

- chaotical behavior:
  $D_u = 1\cdot 10^{-5}$, $D_v = 1\cdot 10^{-5}$, $F = 0.025$, $k = 0.05$, $L = 0.5$
- traveling waves:
  $D_u = 2\cdot 10^{-5}$, $D_v = 1\cdot 10^{-5}$, $F = 0.025$, $k = 0.0544$, $L = 0.5$

First, we performed quantitative comparison of numerical solutions by nonlinear Galerkin schemes (nomat, tridiag) with finite difference scheme (fdm) for the Gray-Scott model. For results given by the selected initial setup and mesh size of 401 grid nodes see Fig. 2. Both components of the solution, u and v are depicted. The nonlinear Galerkin schemes are capable of reproducing the patterns obtained from the finite difference method up to certain time. We can see that up to the time $t = 2000$ the quantitative behavior of numerical schemes under comparison is the same. Difference in solutions starts to be visible at later times. For finer meshes we can conclude that the quantitative behavior was the same for longer times. For more accurate comparison, see measurement of computational efficiency of these numerical approaches below.

Next, we performed CPU time comparison. In agreement with results in [12] and results referenced in [5] we observed savings in CPU time requirements for numerical scheme (34) - (39) in comparison to (40) - (45). This may be in part by reduction of the size of the evolution problem and computationally cheap evaluation of corrections x_{2i+1}, w_{2i+1} in (32).

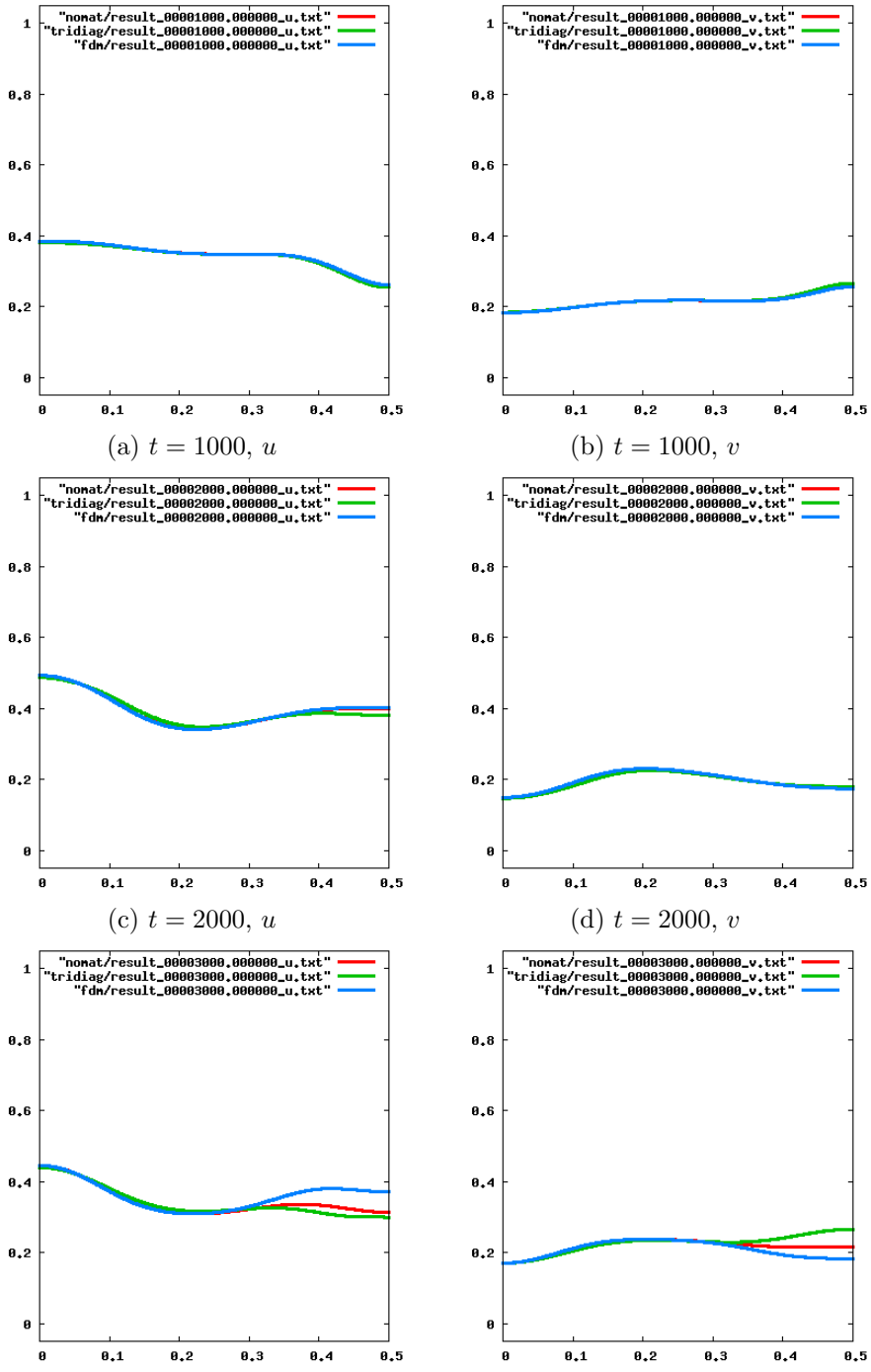

(a) $t = 1000$, u (b) $t = 1000$, v

(c) $t = 2000$, u (d) $t = 2000$, v

(e) $t = 3000$, u (f) $t = 3000$, v

Figure 2: Quantitative comparison of numerical solutions by nonlinear Galerkin schemes (nomat, tridiag) with finite difference scheme (fdm) for the Gray-Scott model. Solution dynamics: Chaotical behavior. Numerical grid size $n = 401$.

method	*Runtime* (*s*)	speedup
fdm	63.766	100.00%
nomat	26.173	41.05%
tridiag	163.771	256.83%

(a) $n = 3201$.

method	*Runtime* (*s*)	speedup
fdm	573.315	100.00%
nomat	222.558	38.82%
tridiag	1353.094	236.01%

(b) $n = 6401$.

Table 1: Computational times of NLG schemes (nomat, tridiag) relative to the computational time of the FDM scheme. Gray-Scott model. Solution dynamics: Chaotical behavior.

method	*Runtime* (*s*)	speedup
fdm	0.504	100.00%
nomat	0.288	45.38%
tridiag	1.499	297.24%

(a) $n = 401$.

method	*Runtime* (*s*)	speedup
fdm	15.116	100.00%
nomat	6.973	46.13%
tridiag	41.963	277.60%

(b) $n = 1601$.

Table 2: Computational times of NLG schemes (nomat, tridiag) relative to the computational time of the FDM scheme. Gray-Scott model. Solution dynamics: Traveling waves.

Depending on the parameter values in the Gray-Scott model we observed reduction of the computational time to 70%-40% of the reference time for the finite difference scheme, see Tab. 1 and Tab. 2 for example results. For completeness the measurement results for the numerical scheme involving solution of the linear systems (32) - (33) are included.

Results for the simplified problem (47) and particular parameters $D = 1 \cdot 10^{-3}$, $k = 10.0$, $\alpha = 1.0$, $\gamma = 0.2$ are given in Tab. 3. Here, reduction of the computational time to 35% of the the reference time for the finite difference scheme was achieved for the the finite element nonlinear Galerkin scheme (34) - (39).

We also performed measurement of the computational efficiency. We measured computational times required to reach given approximation error in numerical solution. The error was measured in L_2 and L_∞ norms. We present comparison of finite difference scheme (40) - (45) and nonlinear Galerkin schemes (34) - (39), (32) - (33).

In case of the measurement for the Gray-Scott reaction-diffusion system we used finite difference numerical approximation by the scheme (40) - (45) computed on fine grid as a reference solution for the error measurement. Example results of the measurement in logarithmic scale are plotted in Fig. 3. Here we performed measurement for the

method	*Runtime* (*s*)	speedup
fdm	144.997	100.00%
nomat	50.410	34.77%
tridiag	168.004	115.87%

(a) $n = 401$.

method	*Runtime* (*s*)	speedup
fdm	1161.180	100.00%
nomat	405.543	34.93%
tridiag	1341.317	115.51%

(b) $n = 801$.

Table 3: Computational times of NLG schemes (nomat, tridiag) relative to the computational time of the FDM scheme. Problem with analytical solution. Parameter values: $D = 1 \cdot 10^{-3}$, $k = 10.0$, $\alpha = 1.0$, $\gamma = 0.2$.

chaotical behavior dynamics and measured computational times and approximation error at particular model time $t = 350$. On the horizontal axis we plotted computational times and on the vertical axis we have errors in the numerical solutions. This measurement includes simulations for various numerical grid sizes from $n = 201$ up to $n = 6401$. Reference solution was computed on numerical grid with $n = 12801$ grid nodes. With refining numerical grid we see rise in computational times and increase in precision of the numerical approximation. We see that in this particular measurement the computational efficiency of finite difference scheme (40) - (45) and finite element nonlinear Galerkin scheme (34) - (39) appears to be the same.

The plot Fig. 3 looks similar when changing the reference solution for the one by the nonlinear Galerkin scheme (34) - (39). We could see similar results also for different parameter values in the Gray-Scoot model.

The same measurement was performed for the problem (47) and parameter values $D = 1 \cdot 10^{-3}$, $k = 10.0$, $\alpha = 1.0$, $\gamma = 0.2$. Plot of computational efficiency for model time $t = 400$ in logarithmic scale are given in Fig. 4. Similar results were obtained for measurements at different model times. Here the finite element nonlinear Galerkin scheme (34) - (39) appears to have better computational efficiency.

Next, we performed measurement of the experimental order of convergence (EOC) for numerical schemes under comparison. To compute EOC coefficients α_{EOC}, we use equation

$$\frac{\|u - u_{h_1}\|}{\|u - u_{h_2}\|} = \left(\frac{h_1}{h_2}\right)^{\alpha_{EOC}}, \tag{48}$$

where u denotes the analytic (reference) solution, u_{h_1} and u_{h_2} are numerical approximations of the solution for the numerical grids with mesh parameters h_1, h_2. We use L_2 and L_∞ norms

$$\begin{aligned} \|u - u_h\|_{L_\infty} &= \max_i \left\{|u^i - u_h^i|\right\}, \\ \|u - u_h\|_{L_2} &= \sqrt{\sum_i h|u^i - u_h^i|^2}. \end{aligned}$$

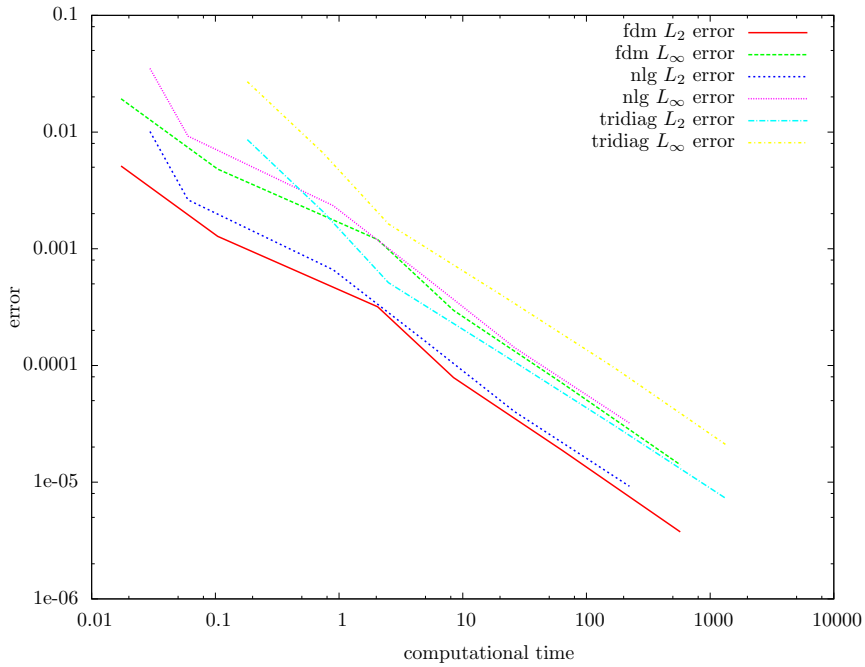

Figure 3: Computational efficiency of nonlinear Galerkin schemes (nomat, tridiag) in comparison to finite difference scheme (fdm) scheme for the Gray-Scott model. Model dynamics: Chaotical behavior. Model (dimensionless) time $t = 350$. Logarithmic scale.

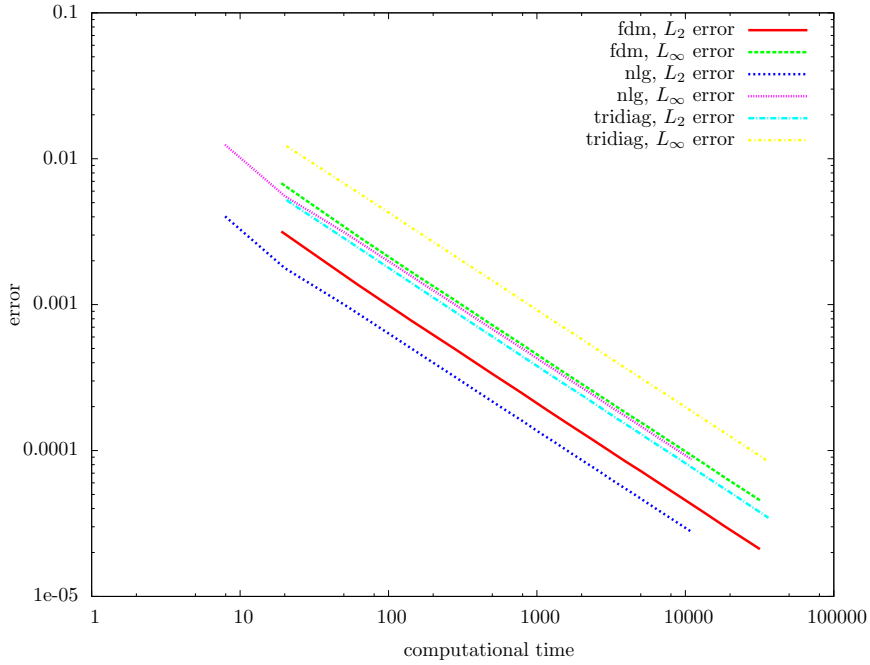

Figure 4: Computational efficiency. Simplified reaction-diffusion equation with analytical solution. Parameter values $D = 1 \cdot 10^{-3}$, $k = 10.0$, $\alpha = 1.0$, $\gamma = 0.2$. Model (dimensionless) time $t = 400$. Logarithmic scale.

		fdm			
N_x	h	EOC L_2	EOC L_∞	error L_2	error L_∞
00201	-	-	-	-	-
00401	1.2500e-03	+2.0438	+2.0507	+6.7750e-04	+1.7759e-03
00801	6.2500e-04	+2.0152	+2.0167	+1.6760e-04	+4.3886e-04
01601	3.1250e-04	+2.0198	+2.0202	+4.1328e-05	+1.0819e-04
03201	1.5625e-04	+2.0711	+2.0711	+9.8352e-06	+2.5747e-05
		nlg			
N_x	h	EOC L_2	EOC L_∞	error L_2	error L_∞
00201	-	-	-	-	-
00401	1.2500e-03	+1.9930	+2.0179	+8.3103e-03	+1.8936e-02
00801	6.2500e-04	+2.0247	+2.0427	+2.0423e-03	+4.5959e-03
01601	3.1250e-04	+2.0089	+2.0126	+5.0743e-04	+1.1390e-03
03201	1.5625e-04	+2.0051	+2.0023	+1.2641e-04	+2.8429e-04
		tridiag			
N_x	h	EOC L_2	EOC L_∞	error L_2	error L_∞
00201	-	-	-	-	-
00401	1.2500e-03	+1.9971	+2.0467	+8.1387e-03	+1.9977e-02
00801	6.2500e-04	+2.0300	+2.0585	+1.9928e-03	+4.7958e-03
01601	3.1250e-04	+2.0103	+2.0170	+4.9464e-04	+1.1849e-03
03201	1.5625e-04	+2.0052	+2.0034	+1.2321e-04	+2.9554e-04

Table 4: Tables of EOC coefficients and errors in numerical solution measured for the Gray-Scott model and nonlinear Galerkin schemes (nomat, tridiag) in comparison to finite difference scheme (fdm). Model dynamics: Chaotical behavior.

For each norm in the fraction on the left-hand side we first search for its maximum within time interval $[T_1, T_2]$ for given $0 < T_1 < T_2$. Finally, the *EOC* is the average of *EOC* coefficients α_{EOC} computed for individual mesh parameters.

In Tab. 4 we see *EOC* coefficients α_{EOC} we measured for the Gray-Scott model exhibiting chaotical behavior. Numerical results between times $T_1 = 300$, $T_2 = 350$ were used for the measurement. As a reference solution u in (48) we used solution by the finite difference scheme (40)-(45) computed on the fine grid with $n = 12801$ nodes.

In Tab. 5 we see *EOC* coefficients α_{EOC} measured for the problem (47) with known analytical solution for parameter values $D = 1 \cdot 10^{-3}$, $k = 10.0$, $\alpha = 1.0$, $\gamma = 0.2$. Numerical results between times $T_1 = 900$, $T_2 = 1000$ were used for the measurement.

In both *EOC* measurements, similar results were obtained for different time intervals within the maximum time interval $[0, 1000]$ which was used for simulations.

6. Conclusion

In this paper we applied finite element nonlinear Galerkin method to the solution of selected reaction-diffusion equations in one spatial dimension and compared numerical results with those obtained by the finite difference method. We showed reduction of the CPU time requirements as an advantage of the finite element nonlinear Galerkin method. On the other hand, the nonlinear Galerkin scheme (34)-(39) seems to be less accurate then the standard finite difference scheme (40)-(45) on the same grid. This can be compensated by a slight increase of the grid size. Experimental order of convergence of tested numerical scheme is the same according to our measurements. Future work is application of the finite element nonlinear Galerkin method to particular problems in two spatial dimensions.

Acknowledgment

Partial support of the project of "Nečas Center for Mathematical modeling", No. LC06052, of the project "Applied Mathematics in Physics and Technical Sciences", No. MSM6840770010 of the Ministry of Education, Youth and Sports of the Czech Republic and of the project "Advanced Control and Optimization of Biofuel Co-Firing in Energy Production", project No. TA01020871 of the Technological Agency of the Czech Republic is acknowledged.

References

[1] Dkhil F., Logak E. and Nishiura Y.: Some analytical results on the Gray-Scott model, in: *Asymptotic Analysis*, Vol. **39**, No. 3-4, (2004) 225–261, IOS Press.

[2] Doelman A.: Pattern formation in the one-dimensional Gray-Scott model, in: *Nonlinearity*, Vol. **10**, (1997) 523–563, IOP Publishing.

[3] Gray, P. and Scott S.K.: Autocatalytic reactions in the isothermal, continuous stirred tank reactor: oscillations and instabilities in the system $A + 2B \to 3B$, $B \to C$, in: *Chem. Eng. Sci.*, Vol. **39**, No. 6 (1984) 1087–1097, Elsevier Science.

		fdm			
N_x	h	EOC L_2	EOC L_∞	error L_2	error L_∞
00201	-	-	-	-	-
00301	1.6667e-03	+2.0499	+2.0449	+2.0093e-03	+4.3988e-03
00401	1.2500e-03	+2.0237	+2.0213	+1.1225e-03	+2.4592e-03
00601	8.3333e-04	+2.0119	+2.0106	+4.9651e-04	+1.0883e-03
00801	6.2500e-04	+2.0058	+2.0052	+2.7882e-04	+6.1125e-04
01201	4.1667e-04	+2.0030	+2.0026	+1.2377e-04	+2.7138e-04
01601	3.1250e-04	+2.0015	+2.0013	+6.9592e-05	+1.5259e-04
02001	2.5000e-04	+2.0009	+2.0007	+4.4530e-05	+9.7645e-05
		nlg			
N_x	h	EOC L_2	EOC L_∞	error L_2	error L_∞
00201	-	-	-	-	-
00301	1.6667e-03	+2.0229	+1.9951	+1.9491e-03	+5.9125e-03
00401	1.2500e-03	+2.0127	+1.9976	+1.0924e-03	+3.3281e-03
00601	8.3333e-04	+2.0066	+1.9988	+4.8421e-04	+1.4799e-03
00801	6.2500e-04	+2.0018	+1.9994	+2.7223e-04	+8.3257e-04
01201	4.1667e-04	+2.0009	+1.9997	+1.2094e-04	+3.7008e-04
01601	3.1250e-04	+2.0004	+1.9998	+6.8022e-05	+2.0818e-04
02001	2.5000e-04	+2.0003	+1.9999	+4.3532e-05	+1.3324e-04
		tridiag			
N_x	h	EOC L_2	EOC L_∞	error L_2	error L_∞
00201	-	-	-	-	-
00301	1.6667e-03	+2.0677	+2.0155	+2.8739e-03	+6.6725e-03
00401	1.2500e-03	+2.0323	+2.0067	+1.6016e-03	+3.7460e-03
00601	8.3333e-04	+2.0166	+2.0032	+7.0704e-04	+1.6627e-03
00801	6.2500e-04	+2.0085	+2.0015	+3.9674e-04	+9.3486e-04
01201	4.1667e-04	+2.0046	+2.0008	+1.7600e-04	+4.1536e-04
01601	3.1250e-04	+2.0025	+2.0004	+9.8928e-05	+2.3362e-04
02001	2.5000e-04	+2.0016	+2.0002	+6.3291e-05	+1.4951e-04

Table 5: Tables of EOC coefficients and errors in numerical solution measured for the problem with analytical solution (47) and nonlinear Galerkin schemes (nomat, tridiag) in comparison to finite difference scheme (fdm). Parameter values $D = 1 \cdot 10^{-3}$, $k = 10.0$, $\alpha = 1.0$, $\gamma = 0.2$.

[4] He Y.N., Hou Y.R. and Mei L.Q.: Global Finite Element Nonlinear Galerkin Method for the Penalized Navier-Stokes Equations, in: *J. Comp. Math.*, Vol. **19**, No. 6 (2001) 607–616, Global Science Press.

[5] Marion, M. and Temam R.: Nonlinear Galerkin Methods, in: *SIAM Journal on Numerical Analysis*, Vol. **26**, No. 5 (1989) 1139–1157, Society for Industrial and Applied Mathematics.

[6] Marion, M. and Temam R.: Nonlinear Galerkin Methods: The Finite Element Case, in: *Numerische Mathematik*, No. 57 (1990) 205–226, Springer Berlin / Heidelberg.

[7] Marion M. and Xu J.: Error Estimates on A New Nonlinear Galerkin Method Based on Two-grid Finite Elements, in: *SIAM Journal on Numerical Analysis*, Vol. **32**, No. 4 (1995) 1170–1184, Society for Industrial and Applied Mathematics.

[8] McGough J.S. and Riley K.: Pattern Formation in the Gray-Scott model, in: *Nonlinear Analysis: Real World Application*, Vol. **5**, No. 1 (2004) 1468–1218, Elsevier Science.

[9] Nabh G. and Rannacher R.: A Comparative Study Of Nonlinear Galerkin Finite Element Methods For Dissipative Evolution Problems, preprint, 1996, IWR Heidelberg.

[10] Nishiura Y. and Ueyama D.: Spatio-temporal chaos for the Gray-Scott model, in: *Physica D: Nonlinear Phenomena*, Vol. **150**, No. 3-4 (2001) 137–162, Elsevier Science.

[11] Nishiura Y. and Ueyama D.: Self-Replication, Self-Destruction, and Spatio - Temporal Chaos in the Gray-Scott model, in: *Forma*, Vol. **15**, (2000) 281–289, Scipress.

[12] Šembera J. and Beneš M.: Nonlinear Galerkin Method for Reaction - Diffusion Systems Admitting Invariant Regions, in: *Journal of Comp. and Appl. Math.*, Vol. **136**, No. 1-2 (2001) 163–176, Science Direct.

[13] Wei J. and Winter M.: Asymmetric spotty patterns for the Gray-Scott model in $\mathbb{R}^2$, in: *Stud. Appl. Math.*, Vol. **110**, No. 1 (2003) 63–102, Blackwell.

[14] Wei J.: Pattern formation in two-dimensional Gray-Scott model: existence of single-spot solutions and their stability, in: *Physica D: Nonlinear Phenomena*, Vol. **148**, No. 1-2 (2001) 20–48, Science Direct.

Jan Mach
Czech Technical University in Prague, Faculty of Nuclear Sciences and Physical Engineering, Department of Mathematics, Trojanova 13, Prague 2, 120 00
E-mail: jan.mach(at)fjfi.cvut.cz